International Journal of Pure and Applied Mathematics

Volume 10 No. 2 2004, 205-220

TOPOLOGICAL INVARIANTS OF A CHAOTIC PENDULUM

M. Mercês Ramos[1], C. Correia Ramos[2]
R. Severino3, J. Sousa Ramos[4] §

[1]Lisbon Higher School of Education (ESELx)
Polytechnical Institute of Lisbon
1549-003 Lisbon, PORTUGAL
e-mail: mercesr@eselx.ipl.pt

[2]Department of Mathematics
University of Évora
Rua Romäo Ramalho, 59 - 7000 Évora, PORTUGAL
e-mail: ccr@uevora.pt

[3]Department of Mathematics
University of Minho
Campus de Gualtar, 4710-057 Braga, PORTUGAL
e-mail: ricardo@math.uminho.pt

[4]Department of Mathematics
Technical University of Lisbon
Av. Rovisco Pais 1, 1049-001 Lisbon, PORTUGAL
e-mail: sramos@math.ist.utl.pt

Abstract: We identify a region of the parameter space for which the study of periodically driven damped pendulum motions can be reduce to iterates of one-dimensional maps. Being so, we can use symbolic dynamics to define and compute the topological entropy of a pendulum dynamics and study its change with the damping and forcing parameters. Finally, we introduce and compute a second topological invariant in order to distinguish isentropic solutions.

Received: November 11, 2003

§Correspondence author

AMS Subject Classification: 37C15, 37B10, 37B40, 37B55
Key Words: topological invariants, symbolic dynamics, topological entropy, pendulum, chaos

1. Introduction and Preliminaries

Unwanted oscillations has always been around, either in physical systems, or in engineering devices. Looking back, we can clearly see that it was the lack of a model to simulate and of mathematics to describe that fundamentally prevent physicists and engineers to understand the nature of these oscillations and, in some cases, the ability to control them. Since differential equations are the mathematical model widely used for both natural phenomena and engineering systems, one can easily understand why the study of the complexity of its solutions, albeit its enormous difficulty, has been one of the most exciting subjects of research for the last two decades. However, one can say without much controversy that the present knowledge and understanding of what is known as chaotic behavior is essentially due to the study of simple discrete dynamical systems. From numerical experiments and, sometimes, subsequent rigorous analysis, to the sophisticated techniques of symbolic dynamics, it has been the iteration of maps in the interval that has allowed us to characterize the dynamical complexity of deterministic chaos. In modern theory of dynamical systems the concept of topological invariants is particularly relevant, since they are the main tool to distinguish and classify a priori similar complicated dynamical behavior. The main purpose of this work is to characterize a class of solutions of the forced damped pendulum model via topological invariants introduced for cubic maps of the interval.

To accomplish that we start by identifying a region of the parameter space for which the observed chaotic physical phenomena can be approximately modelled by the iteration of a cubic map in the interval, allowing us to take advantage of the theory of modal maps on the interval, see Milnor-Thurston and Collet-Eckmann.

2. The Forced Damped Pendulum Model

The planar pendulum subject to frictional damping and a driving sinusoidal force is not only a matter of technological interest, but also of fundamental importance. According to Newton Law, its motion can be described by the

second order non-autonomous ordinary differential equation

$$m\ell^2\ddot{\theta} + \gamma\dot{\theta} + mg\ell\sin\theta \;=\; B\cos(\omega t),$$

with θ the angle of the pendulum with respect to the vertical, so that $\theta = 0$ corresponds to straight down. This model includes friction and gravity, which pulls the pendulum bob down, as well as an external force which keeps accelerating the bob clockwise and counterclockwise. This periodic forcing, constantly providing energy to the pendulum, guarantees that the pendulum will keep swinging, provided the amplitude B is nonzero. As usual we will assume that the pendulum is free to swing through 360 degrees, therefore θ and $\theta+2\pi$ should be considered the same position of the pendulum (for plotting purposes it is convenient to keep θ in the range $[-\pi, \pi]$). In order to get a simpler model, we can suitably choose the system's constants, for which the equation of motion goes like

$$\ddot{\theta} + a\dot{\theta} + \sin\theta \;=\; b\cos(\omega t).$$

This equation has been numerically integrated for different sets of the parameters (a, b, ω) without any problem. The difficulty is that some solutions are so complex that it is not easy to figure out what is going on. Indeed, for large subsets of the parameter space, not only we have no more a regular behavior, but also the pendulum motion can switch rather wildly from regular to complex dynamics with a subtle change of parameters. In fact, the solutions that can occur for the forced damped pendulum illustrates different aspects of chaos: the existence of strange attractors, the presence of several different attracting sets and an extreme sensitivity of the asymptotic motion to initial conditions. For instance, as the driving amplitude b is increased, the occurrence of different transitions between periodic and aperiodic attractors, the coexistence of different attractors, and period-doubling transitions to chaos have been numerically found in real experiments, see Baker-Gollub.

Let us begin by examining the behavior of θ as a function of time for several typical cases. Since θ is an angular variable, values of θ that differs by 2π corresponds to the same position of the pendulum. For plotting purposes it is convenient to keep θ in the range $-\pi$ a π. As we know, with a driving force of zero, the motion is damped and the pendulum comes to rest after a few oscillations. These damped oscillations have a frequency close to the natural frequency of the undamped pendulum, ω_0, and are a vestige of simple harmonic motion. With a small driving force, with $a = 0.5$, we find two regimes: the first few oscillations are affected by the decay of an initial transient motion as is the case of no driving force. That is, the initial displacement of the pendulum

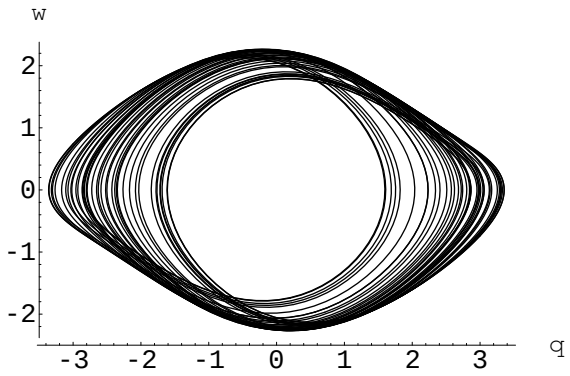

Figure 1: Orbit $(\theta(t), \omega(t)) = (w, q)$ for $a = 0.5, b = 1.1$

leads to a component of the motion that decays with time and has an angular frequency of $\approx \omega_0$. After this transient motion is damped away, the pendulum settles into a steady oscillation in response to the driving force. The pendulum motion has an angular drive frequency, ν, different from the 'natural' angular frequency ω_0 and an amplitude determined by the interplay between the energy added by the driving force and the energy dissipated by the friction. With a small driving force the trajectory in phase-space (θ, ω) space quickly settles into a regular orbit in phase space corresponding to the oscillatory motion of both θ and ω. It can be shown that this final orbit is independent of the initial conditions.

The behavior change radically, for the same value, $a = 0.5$, when the driving force is increased to $b = 1.1$. Now the motion is no longer simple, even at long time. In Figure 1, we plot the angular velocity ω as a function of θ, a phase-space plot. While this pattern is certainly not a simple one it is not completely random. The behavior in the chaotic regime the phase-space trajectories exhibit many orbits that are nearly closed but are not. This is a common property of chaotic systems - they generally exhibit phase-space trajectories with significant structure.

The Poincaré section technic can be used to reduce the dimensionality of the phase space and so make the analysis simpler. Now we focus on the construction of a Poincaré section. For a three-dimensional state space, the Poincaré section is generated by choosing a Poincaré plane, or a two-dimensional surface, and recording on that surface the points at which a given trajectory cuts through that surface. For autonomous systems, such as the damped driven pendulum model equations, we choose some convenient plane in the phase space. When a

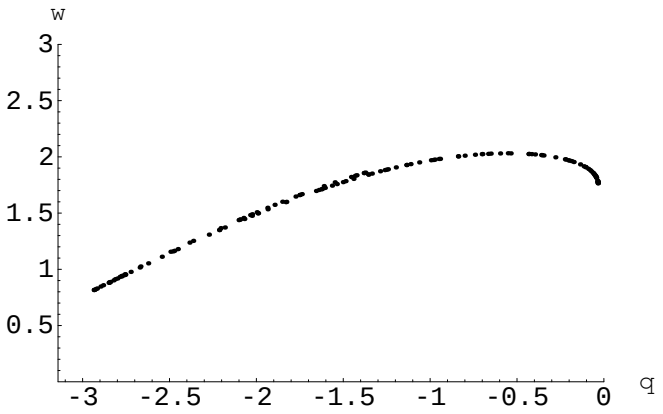

Figure 2: Poincaré map for $a = 0.5, b = 1.1$

trajectory crosses that plane passing from, for example, positive ω to negative ω values, we record that crossing point. As the system has a natural period associated with it, say the period of a driving force, then the Poincaré section could be a surface corresponding to a definite (but arbitrarily chosen) phase of that force, that is, we only display the point when $\nu t = n\pi$, with n integer. In the latter case the Poincaré section is analogous to a "stroboscopic portrait". We can applied this to the pendulum by observing the behavior, and recording the values of θ and ω, at a rate that matches the drive frequency, and this is effectively what we have done in the Poincaré section shown in Figure 2. It is easy to verify that in the nonchaotic regime, with $a = 0.5$ and $b = 0.5$, it would yield a single point (after allowing the initial transient to decay), since at any particular point of the drive cycle we would always find the same values of θ and ω. In the chaotic regime, the result of such a stroboscopic plot is very different. It turns out that except for the initial transient motion this trajectory exhibits the same aspect for a wide range of initial conditions.

In a large number of cases the Poincaré map reduce to a one-dimensional iterated map. In general, we need to know both coordinates (say, θ and ω) of one trajectory intersection point on the plane, as well as the map, to be able to predict the location of the next intersection point. However, in some cases, the system behaves in such a way that less information is required. For example, we may need to know only ω_n in order to be able to predict θ_n. In this case the mapping functions can be written as

$$\begin{cases} \omega_n = P_\omega(\theta_n)\,, \\ \theta_{n+1} = P_\theta(\theta_n, P_\omega(\theta_n))\,, \end{cases} \qquad \Rightarrow \theta_{n+1} = f_{a,b}(\theta_n)\,,$$

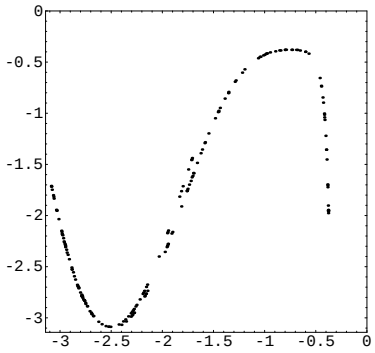

Figure 3: Cubic like map

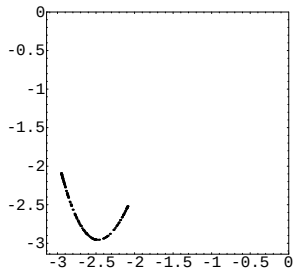

Figure 4: Quadratic map

where a and b are the parameters.

Figure 3 shows the return map plotted for the angular velocity of the driven damped pendulum with $\nu = 2/3$, $a = 0.5$ and $b = 1.09$ which yields chaotic behavior. The return map indicates that for this set of parameter values, the behavior of the θ coordinate can be modeled by a one-dimensional iterated map. For further information, see the references [4], [3].

This paper is organized as follows. We first define a region, $\Re$, in the a, b space, for a set of parameter values in which the behavior of the θ coordinate, in the return map, can be approached by a one-dimensional iterated map (see Figure 3). In Section 2 we identified, in region $\Re$, periodic behavior and chaotic behavior, represented by a quadratic or a cubic function. The entropy is calculated for different sets of parameters, in $\Re$, for which the Poincaré map is approached by a quadratic or a cubic map, and we analyze the variation of the entropy with damping parameter, a, and the forcing parameter, b. In Section 3, to distinguish isentropic motions we introduce a new topological invariant

and we study some of its properties.

In the present paper a procedure to quantify the topological complexity of a physical system depending on parameters is described. The scheme consists on finding the periodic hyperbolic points of Poincaré map corresponding to the dynamical system and the calculation of the topological invariants. This procedure is applied to the case of the chaotic pendulum at some region $\Re$ in the space of parameters. We calculate the variations of topological entropy of the dynamical system in the region $\Re$. However outside the region considered the topological entropy are not yet calculated. To obtain these values will be the purpose of future studies. Nevertheless the entropy and the new topological quantity, that we denote by r, to distinguish different systems with equal topological entropy, allow to study quantitative measures of its orbit complexity. As such, they are important invariants to know.

3. Poincaré Map in the Region $\Re$ and Entropy of Chaotic States

We can reduce, in a convenient region $\Re$ of the parameters, the study of the motions of the pendulum to the iterates of 2-parameters family of functions f_{ab} in the interval $I = [-\pi, 0]$.

We define the region $\Re$ as:

$$\Re = \{(a, b) \in R^2 : -\pi \leq f_{ab}(c_i) \leq 0, i = 1, 2\},$$

where c_i are the critical points, see Figure 5. In this region the map f_{ab} is like a cubic map and we impose that the critical points stay in the interval [-π, 0], see Figure 3.

Programing conveniently the map f_{ab}, of the first return to the interval I and changing a, b in the region $\Re$ we have all the diversity of orbits and bifurcations that occur in the 2-parameters family with two critical points as in the cubic (bimodal) map family. Nevertheless for special subsets of $\Re$ and choosing the initial conditions properly the motion of the pendulum reduces to iterates of a quadratic map, see Figure 4.

The infinite diversity of motions and bifurcation that occur as motions of the pendulum become visible in bifurcations diagrams, see Figure 6 and Figure 7.

The exhaustive and rigorous approach becomes possible with the technics of symbolic dynamics as we will see below.

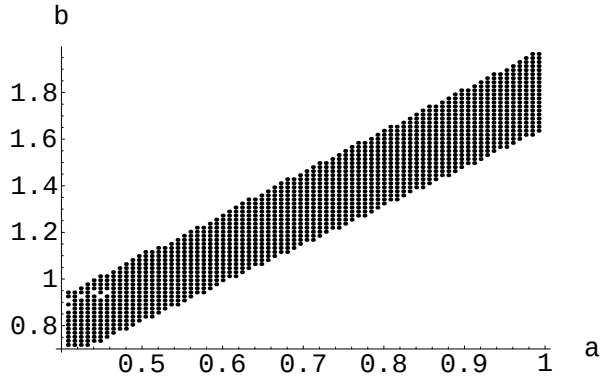

Figure 5: Region $\Re$

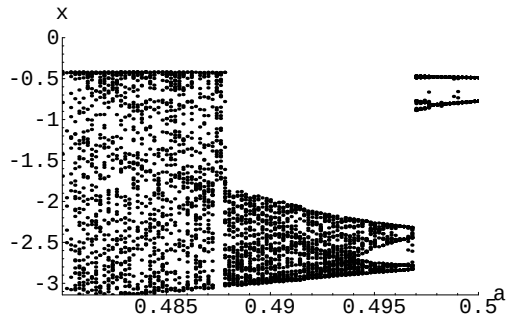

Figure 6: Bifurcation diagram for $b = 1.075$

For the study of two parameter families $f_{a,b}$ of maps of the interval with two critical points, i.e. bimodal maps of the interval see [11], [9], [10]. To each value (a, b) of the parameters $f_{a,b}\colon I \to I$, from the closed interval I to itself, is piecewise monotone and I is subdivided in three subintervals: $L = [c_0, c_1[$, $M =]c_1, c_2[$ and $R =]c_2, c_3]$, where c_i is the critical points or the extremum points, in such a way that the restriction of f to each interval is strictly monotone. Thus the restriction of f to the subinterval L and R, i.e. $f_{a,b|L}$ and $f_{a,b|R}$ are decreasing and $f_{a,b|M}$ is increasing.

On the other hand for each value (a, b) we define the orbits of the critical points by:

$$O(c_i) = \{x_j^{(i)} : x_j^{(i)} = f^j(c_i),\ j \in \mathbb{N}\}\,,$$

with $i = 1, 2$. With the aim of studying the topological properties of these orbits we associate to each orbit $O(c_i)$ a sequence of symbols $S = S_1 S_2 \ldots S_j \ldots$, where

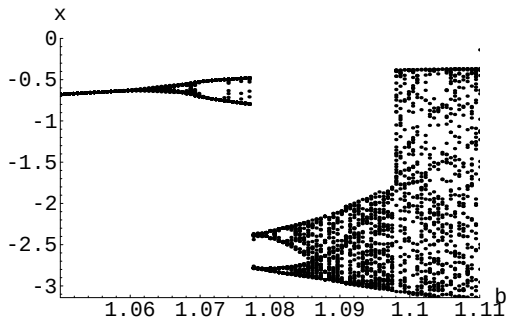

Figure 7: Bifurcation diagram for $a = 0.5$

for each c_i, we have $S_j = L$ if $f^j_{a,b}(c_i) < c_1$, $S_j = A$ if $f^j_{a,b}(c_i) = c_1$, $S_j = M$ if $c_1 < f^j_{a,b}(c_i) < c_2$, $S_j = B$ if $f^j_{a,b}(c_i) = c_2$ and $S_j = R$ if $f^j_{a,b}(c_i) > c_2$. If we denote by n_{LR} the number of the symbols L and R in a finite subsequence of S we can define the LR-parity of this subsequence according to whether n_{LR} is even or odd. In what follows we define an order relation in $\Sigma_5 = \{L, A, M, B, R\}^{\mathbb{N}}$ that depends on the LR-parity (see [9]).

Let V be a vector space of three dimension defined over the rationales having as a basis the formal symbols $\{L, M, R\}$, then to each sequence of symbols $S = S_1S_2 \dots S_j \dots$ we can associate a sequence $\theta = \theta_0 \dots \theta_j \dots$ of vectors from V, setting $\theta_j = \prod_{i=0}^{j-1} \epsilon(S_i)S_j$, with $j > 0$, $\theta_0 = S_0$, when $i = 0$ and $\epsilon(L) = \epsilon(R) = -1 = -\epsilon(M)$, where to the symbols corresponding to the critical point c_1 and c_2 we associate the vector $\frac{L+M}{2}$ and $\frac{M+R}{2}$. Thus $\epsilon(A) = \epsilon(B) = 0$. Choosing then a linear order in the vector space V in such a way that the base vectors satisfy $L < M < R$ we are able to order the sequence θ lexicographically, that is, $\theta < \bar{\theta}$ if and only if $\theta_0 = \bar{\theta}_0, \dots, \theta_{j-1} = \bar{\theta}_{j-1}$ and $\theta_j < \bar{\theta}_j$ for some integer $j \geq 0$. Finally, introducing t as an undetermined variable and taking θ_j as the coefficients of a formal power series θ (invariant coordinate) we obtain $\theta = \theta_0 + \theta_1 t + \ldots = \sum_{j=0}^{\infty} \theta_j t^j$. The sequences of symbols corresponding to periodic orbits of the critical point A and B is $P = AP_1P_2 \dots P_{p-1}A \dots$ and $Q = BQ_1Q_2 \dots Q_{q-1}B \dots$. In what follows we denote by $S^{(k)} = S_1S_2 \dots S_{k-1}C$ the periodic block associated to S, with $C = A$ or B. The realizable itineraries of the critical point c_1 and c_2 for the maps previously defined are called by kneading sequences [9].

Let

$$(y_1, \dots, y_{p+q}) = (c_1, x^{(1)}_1, \dots, x^{(1)}_{p-1}, c_2, x^{(2)}_1, \dots, x^{(2)}_{q-1})$$

be the points corresponding to the periodic orbit of the critical point c_1 and c_2

and call $(z_1, \ldots, z_{p+q})$ the ordered points of these orbits. Under these conditions let ρ be a permutation defined by $(y_1, \ldots, y_n) \to (z_{\rho(1)}, \ldots, z_{\rho(n)})$, where $n = p + q$. In what follows we denote by G_1 the graph, where the vertices $\{z_i\}$, $i = 1, \ldots, n$, are obtained from the permutation matrix ρ associated to the kneading sequence and the edges $\{I_i\}$, $i = 1, \ldots, n-1$, are defined by the pairs (y_i, y_{i+1}). Let C_0 and C_1 be the vector spaces of 0-chains (orbit points) and 1-chains (subintervals) spanned by $\{y_j\}$, $j = 1, \ldots, n$ and by $\{I_i\}$, $i = 1, \ldots, n-1$, respectively. In what follows we use the same symbol for the linear map and their representation matrices. The border of 1-chain is defined from a map $\partial : C_1 \to C_0$, where $\partial I_i = y_{i+1} - y_i$. The incidence matrix of the graph G_1 is given by $\partial = [\partial_{ij}]$, where $\partial_{ij} = \delta_{i+1,j} - \delta_{i,j}$ and $\delta_{i,j}$ is the Kronecker $\delta-$symbol. On the other hand, the shift operator σ takes the form of a rotation $\omega : C_0 \to C_0$ defined by $\omega(z_i) = z_{i+1}$, where $1 \leq i < k$ and $\omega(z_k) = z_1$, for the doubly stable bimodal case. For the stable pair case we have $\omega(u_i) = u_{i+1}$, where $1 \leq i < p$ and $\omega(u_p) = u_1$, $\omega(v_j) = v_{j+1}$, where $1 \leq j < q$ and $\omega(v_q) = v_1$. If we denote by η the product of $\rho\omega\rho^{-1}$, this map induces in C_1 an endomorphism α that is obtained from the commutativity of the following diagram:

$$\begin{array}{ccc} C_1 & \xrightarrow{\partial} & C_0 \\ \downarrow\alpha & & \downarrow\varphi \\ C_1 & \xrightarrow{\partial} & C_0 \end{array}$$

Note that from $\partial\alpha = \varphi\partial$ we could get $\alpha = (\partial^T\partial)^{-1}\partial^T\varphi\partial$, where ∂^T is the transpose matrix of ∂. Note also, that if we neglect the negative signs of the matrix α then this matrix could be obtained as the Markov adjacency matrix associated to the partition $\{I_i\}$ (see [7], [8]). Let's now denote by β a matrix of $(p + q - 1) \times (p + q - 1)$ elements defined by:

$$\beta = \begin{bmatrix} -I_{n_L} & 0 & 0 \\ 0 & I_{n_M+1} & 0 \\ 0 & 0 & -I_{n_R} \end{bmatrix},$$

where I_{n_L}, $I_{n_{M+1}}$ and I_{n_R} are identity matrices of rank n_L, n_{M+1} and n_R, respectively.

Definition 3.1. For each kneading sequence $(P^{(p)}, Q^{(q)}) = (P_1 \ldots P_{p-1}A, Q_1 \ldots Q_{q-1}B)$ or $(P_1 \ldots P_{p-1}\ BQ_1\ \ldots Q_{q-1}A)$ let $U_1 \ldots U_{p+q} = AP_1 \ldots P_{p-1}BQ_1\ \ldots Q_{q-1}$, then we associate a square matrix of $(p+q) \times (p+q)$ elements, $\gamma = [\gamma_{ij}]$ defined by:

$$\begin{array}{ll} \gamma_{i1} = \delta(U_i), & \gamma_{i,i} = \epsilon(U_i), \\ \gamma_{i,p+1} = \nu(U_i), & i = 1, \ldots, p+q, \end{array}$$

where U_i is the i-element of the $p+q$-tuple $(A, P_1, \ldots, P_{p-1}, B, Q_1, \ldots, Q_{q-1})$ and $\delta(R) = \delta(M) = \delta(B) = 1$, $\delta(A) = 0$, $\delta(L) = -1$, $\nu(L) = \nu(M) = \nu(A) = 1$, $\nu(B) = 0$ and $\nu(R) = -1$. And all the other elements of the matrix are zeros.

Proposition 3.1. *The matrix γ introduced before satisfies the following diagram:*

$$\begin{array}{ccccc} C_1 & \xrightarrow{\partial} & C_0 & \xrightarrow{\rho} & C_0 \\ \beta\downarrow & & \downarrow\eta & & \downarrow\gamma \\ C_1 & \xrightarrow{\partial} & C_0 & \xrightarrow{\rho} & C_0 \\ \alpha\downarrow & & \downarrow\varphi & & \downarrow\omega \\ C_1 & \xrightarrow{\partial} & C_0 & \xrightarrow{\rho} & C_0 \end{array}$$

Proof. The proof is as in [7], [8]. □

In what follows we denote by Θ the product of γ by the rotation ω introduced before, that is, $\Theta = \omega\gamma$. Then the characteristic polynomial of the matrix Θ satisfies the next proposition.

Proposition 3.2. *For each kneading sequence $(P_1 \ldots P_{p-1}A, Q_1 \ldots\ Q_{q-1}B)$ or $(P_1 \ldots P_{p-1}\ BQ_1 \ldots Q_{q-1}A)$ we have:*

$$P_\Theta(t) = \det(I - \Theta t) = [1 - \delta(P_1)t - \sum_{i=2}^{p} \delta(P_i)(\prod_{j=1}^{i-1} \epsilon(P_j))t^i]$$
$$\times [1 - \nu(Q_1)t - \sum_{i=2}^{q} \nu(Q_i)(\prod_{j=1}^{i-1} \epsilon(Q_j))t^i] - [\nu(P_1)t + \sum_{i=2}^{p} \nu(P_i)(\prod_{j=1}^{i-1} \epsilon(P_j))t^i]$$
$$\times [\delta(Q_1)t + \sum_{i=2}^{q} \delta(Q_i)(\prod_{j=1}^{i-1} \epsilon(Q_j))t^i]$$

Proof. See [6], [8]. □

This result is important because it is used to prove the next proposition which establishes how the kneading-determinant (see [9]) and the characteristic polynomial of the matrix Θ are related and also because it allows for an easy computation of the topological entropy associated to a map of the interval with one or two critical points (see also [6]). In fact, we have:

Proposition 3.3. *For each kneading sequence $(P_1 \ldots P_{p-1}A, Q_1 \ldots\ Q_{q-1}B)$ or $(P_1 \ldots P_{p-1}BQ_1 \ldots Q_{q-1}A)$ we have:*

$$P_\Theta(t) = (1-t)(1-t^p)(1-t^q)D(t) \text{ or } P_\theta(t) = (1-t)(1-t^{p+q})^2 D(t),$$

where $D(t)$ is the kneading-determinant.

Proof. The proof is similar to the proof given in [6]. □

In what follows let us denote by $\mathcal{M}$ the non-negative matrix defined by $\mathcal{M} = \alpha\beta$. This matrix defines a subshift of finite type that is "equivalent" to the matrix Θ, according to the previous commutative diagram.

Proposition 3.4. *The characteristic polynomial of the matrix θ satisfies the following result:*

$$P_\Theta(t) = (1-t)\det(I - \mathcal{M}\,t).$$

Proof. See [7], [8], [2]. □

To conclude we point out the simplicity of the expression in Proposition 3 which according to Proposition 4 and Proposition 5 allows a simple computation of symbolic invariants of all bimodal maps of the interval, this being important in applications. Note that Θ is directly obtained from the kneading sequence.

Now we study the topological entropy. For the class of systems studied in this paper the topological entropy of $f_{a,b}$, denote by $h_{top}(f_{a,b})$, can be computed by the growth rate of lap number, $s(f)$. Let ℓ_k denote the number of laps of f^k. The topological entropy is then

$$h_{top}(f_{a,b}) = \log\ s(f) = \lim_{k\to\infty} 1/k \log \ell_k$$

($h_{top}(f_{a,b})$ is the logarithm of the growth rate of the number of intervals on which f^k is monotonic, see [12], [9], [10]). Alternatively the topological entropy of the cubic map can be calculated by the spectral radium of the Markov matrix $\mathcal{M}$ (see [6]).

We now explore the behavior of the entropy of the chaotic pendulum with the parameter a, b, i.e., the dependence of $h_{top}(f_{a,b})$ on a,$b \in \Re$, for several cases, as we saw in last section. To each pair of parameters (a, b) is determined a kneading sequence. This kneading sequence determines a Markov partition of the interval which has associated a Markov matrix. The entropy variation comes as the logarithm of the spectral radium of these matrices. In the following we present some calculations.

For the values of the parameters $a = 0.5$ and $b \in [1.088, 1.0969]$ the dynamics is approximately of a quadratic map and for $b \in [1.097, 1.109]$ the dynamics is describe approximately by a cubic map. In these cases the entropy is an increasing function of the forcing parameter b, see Figure 8.

If we fix $b = 1.075$ and $a \in [0.488, 0.4965]$ we have that the entropy is a decreasing function of the damping parameter a, see Figure 9.

We can see that as the parameter a, the damping, increases the behavior of the pendulum, as we should expect, becomes more regular including for certain

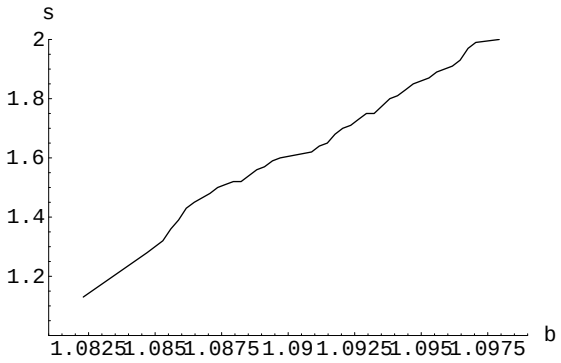

Figure 8: Growth number $s(b)$

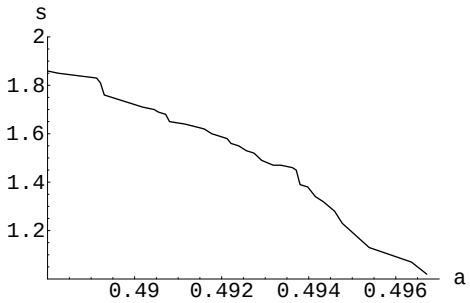

Figure 9: Growth number $s(a)$

values of parameter a that the motion goes to the fixed point. So the entropy as a measure of complexity naturally decreases as the damping a increases.

4. Topological Invariants and Isentropics

The study of topological classification for bimodal maps leads to the introduction of two topological invariants one of them is the growth number $s(f_{a,b}) = e^{h(f_{a,b})}$ and the other number is associated to the relative position of the maximum and the minimum of the map. Our study deals with the properties of these topological invariants related to variation of the parameters a and b. Using the hypothesis $s(f_{a,b}) > 1$ and the Milnor-Thurston results about the topologically semi-conjugate by λ of $f_{a,b}$ to a piecewise linear map $F_{s,r}$ having slope $\pm s(f_{a,b})$ everywhere, we introduce a new topological invariant r to the maps $f_{a,b}$ and we study its properties (see also [1], [13]).

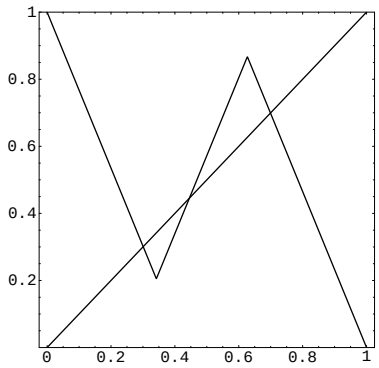

Figure 10: Piecewise linear map for $s = 2.1479...$ and $r = 0.465571...$

There exists one and only one map (see [9]):

$$F_{s,r} : \ [0,1] \to [0,1] \quad \text{so that} \quad F_{s,r}(\lambda(x)) = \lambda(f_{a,b}(x)),$$

for every $x \in I$. This map is piecewise-linear, with slope equal to $\pm s$ everywhere. Let the piecewise-linear map given by:

$$F_{s,r}(y) = \begin{cases} -s\,y + 1 & \text{if} \quad 0 \le y < \lambda(c_1)\,, \\ s\,y + r - 1 & \text{if} \quad \lambda(c_1) \le y < \lambda(c_2)\,, \\ -s\,y + s & \text{if} \quad y \ge \lambda(c_2)\,, \end{cases}$$

where $\lambda(c_1) = \frac{2-r}{2s}$ and $\lambda(c_2) = \frac{1-s-r}{2s}$, see Figure 10.

Then, to each bimodal map $f_{a,b}$ characterized by a kneading sequence $(P^{(p)}, Q^{(q)})$, we can associate two topological invariants. One of them is the growth number $s(f)$, as we saw, and the other is the new invariant given by

$$r(f) = (3+s)/2 - s\,(\lambda(c_1) + \lambda(c_2))\,,$$

with

$$\lambda(c_1) = \sum_{i=1}^{n_L+1} v_i \quad \text{and} \quad \lambda(c_2) = \sum_{i=1}^{n_L+n_M+2} v_i\,,$$

where n_L (resp. n_M) denote the number of symbols L (resp. symbols M) and the vector v is the Perron eigenvector associated to the eigenvalue $\lambda_{\max} = s$, $\mathcal{M}v = \lambda_{\max}\, v$, where $\mathcal{M}$ is the Markov matrix with the extreme intervals $I_0 = [0, z_1]$ and $I_{p+q} = [z_{p+q}, 1]$ include. Note that $r(f)$ is in fact a topological invariant because all the variables $\lambda(c_1)$, $\lambda(c_2)$ and $s(f)$ that lead to

$r(f)$ are topological invariants. On the other hand, this new invariant allow us to distinguish between isentropic dynamics (that is, dynamics with the same entropy). In the piecewise linear case, $F_{s,r}$, the parameter $r(f)$ is the invariant that distinguish isentropic dynamics and $r \in [0, 3-s]$.

Now using previous results we derive our main result.

Theorem 4.1. *The pendulum motions in the $\mathcal{R}$ region can be topological classified by the pair of topological invariants (s, r), where s is the laps growth number ($s(f_{a,b}) = \exp(h(f_{a,b}))$ and r is the invariant given by*

$$r(f_{a,b}) = (3+s)/2 - s(\lambda(c_1) + \lambda(c_2))\,,$$

and λ the map defined by the semi-conjugacy to the piecewise-linear map.

Example 4.1. For the kneading sequence $(P_1P_2P_3BQ_1Q_2A) = (LMMBRMA)$ we can illustrate the result of the previous algorithm calculating the topological invariants associated to this kneading sequence, are $s = 2.1479...$ and $r = 0.465571....$ The Markov matrix

$$\mathcal{M} = \begin{bmatrix} 0 & 0 & 0 & 0 & 1 & 1 & 1 & 1 \\ 0 & 1 & 1 & 1 & 0 & 0 & 0 & 0 \\ 0 & 1 & 0 & 0 & 0 & 0 & 0 & 0 \\ 0 & 0 & 1 & 1 & 1 & 0 & 0 & 0 \\ 0 & 0 & 0 & 0 & 0 & 1 & 0 & 0 \\ 0 & 0 & 0 & 0 & 0 & 0 & 1 & 0 \\ 0 & 0 & 0 & 1 & 1 & 1 & 1 & 0 \\ 1 & 1 & 1 & 0 & 0 & 0 & 0 & 0 \end{bmatrix},$$

with $\mathcal{M}v = \lambda_{\max} v$ the equation of Perron eigenvector. Then we have $\lambda(c_1) = \sum_{i=1}^{2} v_i = 0.357193...$, $\lambda(c_2) = \sum_{i=1}^{6} v_i = 0.624407...$ and $r(f) = (3+s)/2 - s\,(\lambda(c_1) + \lambda(c_2)) = 0.465571....$ The semi-conjugate piecewise-linear map associated to this kneading is given in the Figure 10. The corresponding values of the damping and forcing parameters are $a = 0.50$, $b = 1.10$.

References

[1] P. Almeida, J.P. Lampreia, J. Sousa Ramos, Topological invariants for bimodal maps, In: *European Conference on Iteration Theory, Batschuns*, Set. 13-19, World Scientific, Singapore-New Jersey-Hong Kong (1994).

[2] J.F. Alves, J. Sousa Ramos, Kneading theory: A functorial approach, *Commun. Math. Phys.*, **204** (1999), 89-114.

[3] G.L. Baker, J.P. Gollub, *Chaotic Dynamics: An Introduction*, Cambridge University Press (1996).

[4] J. Gukenheimer, P. Holmes, *Nonlinear Oscillations, Dynamical Systems, and Bifurcations of Vector Fields*, Springer-Verlag, New York (1983).

[5] R.H. Hilborn, *Chaos and Nonlinear Dynamics*, Oxford University Press (1994).

[6] J.P. Lampreia, J. Sousa Ramos, Computing the topological entropy of bimodal maps, In: *Proceedings of ECIT 87*, World Scientific Publishing, Singapore (1989).

[7] J.P. Lampreia, J. Sousa Ramos, Trimodal maps, *Int. J. Bifurcation and Chaos*, **3**, No. 6 (1993), 1607-1617.

[8] J.P. Lampreia, J. Sousa Ramos, Symbolic dynamics for bimodal maps, *Portugaliae Math*, **54**, No. 1 (1997), 1-18.

[9] J. Milnor, W. Thurston, On iterated maps of the interval, In: *Proceedings Univ. Maryland* (Ed. J.C. Alexander), 1986-1987; *Lect. Notes in Math.*, **1342**, Springer-Verlag (1988), 465-563.

[10] J. Milnor, C. Tresser, On entropy and monotonicity for real cubic maps (with an appendix by Adrien Douady and Pierrette Sentenac), *Commun. Math. Phys.*, **209** (2000), 123-178.

[11] C. Mira, *Chaotic Dynamics,* World Scientific, Singapore (1987).

[12] M. Misiurewicz, Szlenk, Entropy of piecewise monotone mappings, *Studia Math.*, **67** (1980), 45-63.

[13] R. Severino, *Invariantes Topológicos e Algébricos em Sistemas Dinâmicos Discretos*, PhD Thesis, Universidade Técnica de Lisboa (2000).